ZIBELINE INTERNATIONAL™ PUBLISHING

ISSN: 2521-5035 (Print)
ISSN: 2521-5043 (Online)
CODEN: ESMACU

Earth Sciences Malaysia (ESMY)

DOI: http://doi.org/10.26480/esmy.01.2025.23.29

CrossMark

RESEARCH ARTICLE

EVALUATION OF HYDROCARBON CONTAMINATION IN GROUNDWATER THROUGH ELECTRICAL RESISTIVITY IMAGING AND GEOCHEMICAL TECHNIQUES

Stanley Uchechukwu Eze[a], Chinemelu, E.S[b]

[a] Department of Applied Geology, Olusegun Agagu University of Science and Technology, Okitipupa, Nigeria
[b] Department of Geology, Federal University of Petroleum Resources, Effurun, 330102, Nigeria
**Corresponding author email: su.eze@oaustech.edu.ng*

ARTICLE DETAILS

Article History:

Received 19 January 2025
Revised 22 February 2025
Accepted 26 March 2025
Available online 11 April 2025

ABSTRACT

The contamination of groundwater by hydrocarbons presents a significant challenge for the residents of the Kegbara Dere community in Ogoniland, Rivers State, Southern Nigeria. The area has been plagued by oil spillage, and the damage done to Ogoniland as a result of oil spillage is so massive that the United Nation (UN) did a report on the extent of pollution in the area. This study aimed to identify and characterize the extent of the groundwater system contamination in the study area. The electrical resistivity imaging and geochemical methods were adopted. 2D electrical resistivity imaging (ERI) along four (4) traverses was processed and analyzed to obtain resistivity-depth sections of the subsurface. Three unique geoelectric zones were delineated, with the intermediate zone identified as the contaminated aquiferous unit. This unit's resistivity values ranged from 10,804 to 100,000 Ωm along line Lx3, 324 to 23,497 Ωm along line Lx5, 1019 to 10,000 Ωm along line Ly6, and from 1000 to 10,000 Ωm along line Ly5 extending from the surface (0.0 m) to depths between 10 m and 20 m and to a profound depth of approximately 40 m. These high resistivity anomalies are characteristic of hydrocarbon contamination since hydrocarbons have a higher electrical resistivity compared to water. This coincides with the depth of the aquifer that serves as the major origin of edible water exploited by the local population and shows that the aquifer system below the study area, usually exploited for groundwater, has been invaded by hydrocarbon contamination plumes. The groundwater specimens from five boreholes were established to have a common total petroleum hydrocarbon (TPH) amount of 739.51 µg/L, above the DPR target and intervention thresholds of 50 and 600 µg/L, respectively. Groundwater specimens with summed polycyclic aromatic hydrocarbons (ΣPAHs) consist of amounts ranging from 0.36 to 1.89 µg/L in BH-1 to 5, that outweigh the DPR target threshold of 0.15 µg/L. Additionally, BTEX concentration was observed in greater levels in the water specimens above the DPR allowance. These findings explain that the area's groundwater is heavily contaminated by dissolved-phase contaminants due to hydrocarbon pollution. The groundwater migration flow route at the spill site shows that the dominant flow direction is towards BH4, located northwest (N-W) of the spill site. A broad characterization of the subsurface as obtained from 2D ERI and geochemical results calls for effective remediation planning at the spill site aided by information about the very possible receptor locations at high possibility of contamination, which was defined in the groundwater flow pattern at the spill site.

KEYWORDS

Hydrocarbon contamination, Electrical resistivity imaging, Geochemical analysis, Groundwater Pollution

1. INTRODUCTION

As global demand for energy has expanded, there has been aggressive exploration and extraction of fossil fuels beneath the surface. These extraction activities frequently cause environmental deterioration through accidents, equipment failure, and blatant sabotage. The Niger Delta is a high-producing hydrocarbon region in southern Nigeria, with a detrimental environmental impact (Obasi and Balogun, 2001; Tamuno and Felix, 2006). Oil slick is the term used to describe the release of a small amount of oil into the environment, whereas oil spill refers to the release of a big amount of oil. The cumulative dynamics of these instances on and beneath the earth's surface frequently alter soil, groundwater, vegetation, and so on (Patel et al., 2019). The major receivers of oil spills, and constantly the most impaired, are the soil, subsoil, surface water, and groundwater. Oil pollution releases harmful chemicals into the environment. These include total petroleum hydrocarbons (TPH), polycyclic aromatic hydrocarbons (PAH), and benzene, toluene, ethylbenzene, and xylene (BTEX). Due to the mobility of hydrocarbons together with their toxicity, mutagenicity, and carcinogenicity, soil contamination is considered a major challenge for healthy environments. These have had a negative impact on the environment and, to a large extent, on groundwater and shallow wells.

Electrical Resistivity Imaging (ERI) provides acceptable results for near-surface examinations and characterizations of polluted sites. Near surface geophysical surveys are conducted at depths of 30 m or less, and the ground is conductive due to the presence of mineral water, various types of rocks, and ground self-potentials caused by dissolved salts. Furthermore, the geoelectrical resistivity approach takes into account pollutants' features such as fluid content, salinity, and ionic content (Telford et al., 1990; Maurya et al., 2017; Olaojo et al., 2018). As a result,

Quick Response Code	Access this article online	
	Website: www.earthsciencesmalaysia.com	DOI: 10.26480/esmy.01.2025.23.29

Cite The Article: Stanley Uchechukwu Eze, Chinemelu, E.S (2025). Evaluation of Hydrocarbon Contamination in Groundwater Through Electrical Resistivity Imaging and Geochemical Techniques. Ethiopia. *Earth Sciences Malaysia, 9(1): 23-29.*

contamination plumes typically respond differently to their environment, and such differences can be detected during contaminant plume characterization. As a result, geophysical methods can distinguish contaminant plume zones from uncontaminated zones in the environment and determine their environmental impact (Slater and Sandberg, 2000).

Nonetheless, the ambiguity suffered from multiple interpretations of geophysical inversion have compelled the need of supplementary information from other causes, alternatively borehole data, to constrain the inversion and confirm its certainty from boreholes in the area to appraise the magnitude f hydrocarbon contamination of groundwater resources, and valuation of groundwater condition on individual health. These steps are essential for the planning of remediation programs at a contamination site (De Vivo et al., 2008).

2. Geology of The Investigation Location

The research location is a hydrocarbon pollution site located at Kegbara-Dere (K-Dere) community in Ogoniland, Gokana local government area of Rivers State. Gokana is positioned amidst latitudes $4^0\,12^1$ and $4^0\,50^1$ North of the equator and between longitudes $7^0\,20^1$ to $7^0\,35^1$ East of the Greenwich meridian (Figure 1). It situates on the Gulf of Guinea and it is about Fifty-four (54) kilometers from Port Harcourt metropolis (Okonny, 2002).

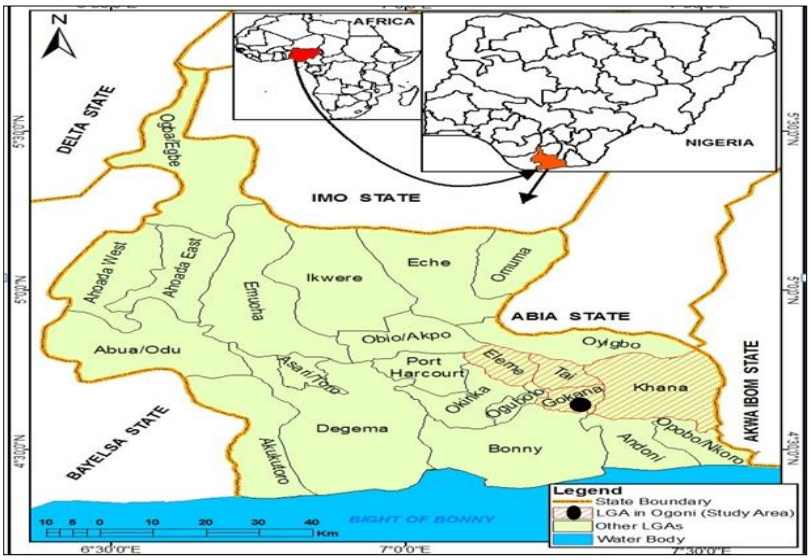

Figure 1: Map displaying Gokana in Ogoni, Rivers State, Nigeria (Source: Rivers State Surveyor General Office, 2016).

The region's geology is concurrent to that of the Niger Delta. The Benin, Agbada, and Akata formations are included in the stratigraphic strata of the Niger Delta Basin (Figure 2). Concise reports of these stratas' emblematic displays have been detailed by the following authors (Doust and Omatsola, 1990; Giadom et al., 2015; Ideozu et al., 2018). The Akata formation is mostly made up of beds of sand and sea-level shale, while it's subsurface is made up of sand and dark gray shale. This bed is valued to be about 7,000 meters thick (Giadom et al., 2015). A series of sandstone and shale deposits make up the upper Agbada formation. Shale is currently in the minor detail, although the top half is originally made up of sand with a slight bit of shale. Benin's upper beds are almost 3,700 m thick and are predominantly uncovered near the coast, but are concealed in manifold locations with lean beds of laterite of variable thickness. It has been recognized as new water-holding sand, and this lithostratigraphic unit (Figure 2) is made up of the aquifers in the delta location (Doust and Omatsola, 1990; Uchegbulam and Ayolabi, 2014).

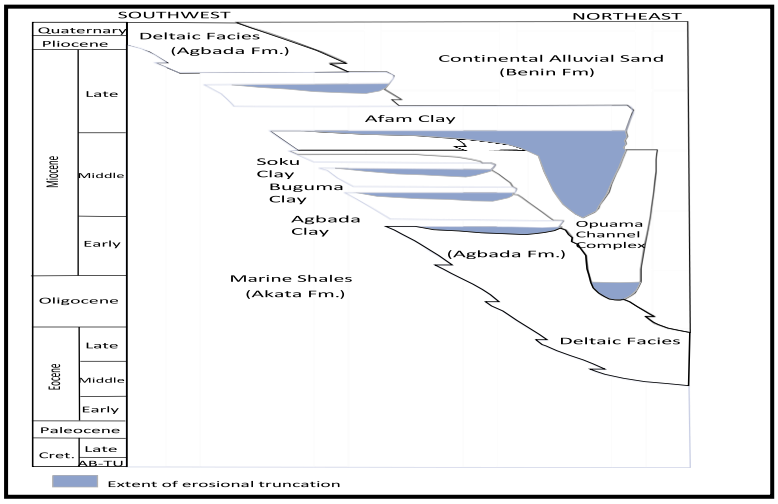

Figure 2: The three stratigraphic units of the Niger Delta (modified from Doust and Omatsola 1990).

3. Materials and Methods

In this study evaluation of hydrocarbon contamination at the pollution site was investigated using 2-D geoelectrical resistivity imaging technique and geochemical method.

3.1 2D Electrical Resistivity Imaging

For the electrical resistivity imaging (ERI) survey, a 200 x 100 m^2 grid was established at the site, and 2D survey profiles were acquired at the spill site. The Wenner-Schlumberger electrode array was used for n-factors 1 through 9 (Pazdirek and Blaha 1996). The n-factor for this array is the fraction of the separation amidst the potential pairs P1-P2 and the original current and potential electrodes C1-P1 according to (Bery, 2016). The ERI survey was made making use of a PASI-16GL resistivity meter with 21 electrodes to facilitate speed in field measurement. The grid lines were arranged to cut across the noted pool of oil spills at the pollution site.

After conducting the 2D ERT survey, the raw data was collated and saved in (.DAT) file format. The Earth-Imager 2D inversion software was utilized to process and invert the 2D apparent resistivity data, to realize the 2D resistivity-depth sections (AGI, 2003).

Figure 3a: Physical Situation of the pollution site as at the time of this study in Kegbara-Dere community, Ogoniland, Rivers State, Southern, Nigeria

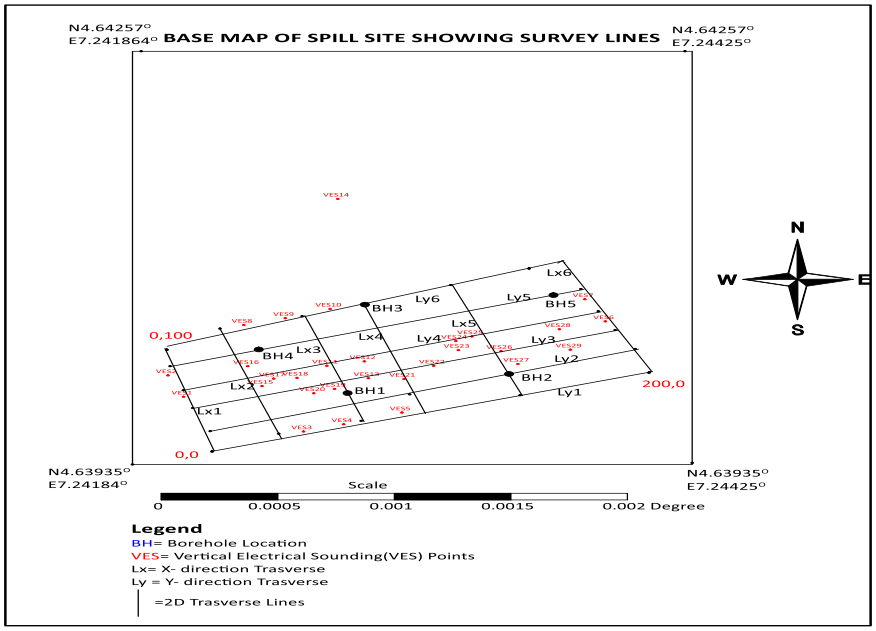

Figure 3b: Base map of data acquisition at the study site in Kegbadere, Ogoniland, Rivers State, showing 2-D grid lines, and borehole points.

3.2 Geochemical Method

Geochemical assessment is a cardinal factor of a valid environmental site-assessment plan, as the information can be utilized to gauge the levels of contaminants in the defiled phase and to substantiate the results of a geophysical field investigation. In this study, five (5) boreholes were bored at the oil spill site along 2D resistivity lines Lx3, Lx4, Lx5, and Ly5 (Figure 3b). The Boreholes were each penetrated to a depth of 10.0 m. Groundwater specimens were gathered from each of the boreholes by means of a sample vial hooked to a weight.

The specimens are ideal representation of water from the boreholes because the water table within the study area is roughly less than 6 m.

Each borehole's depth to the water table and ground altitude were determined. A migration flow contour map was constructed by removing the ground altitude from the depth to the water table, which is noted as the hydraulic head (Table 1).

Table 1: Elevation, Water Level and Hydraulic Heads of Five (5) Boreholes

Borehole No.	Surface-altitude (m)	Static Water Level (m)	Hydraulic Head (m)
BH-1	22.8	2.54	20.26
BH-2	20.5	2.77	17.73
BH-3	19.0	3.38	15.62
BH-4	15.66	2.89	12.77
BH-5	21.50	2.27	19.23

The samples' geochemical study was done following the standard setting. The hydrocarbon contaminants appraised include total petroleum hydrocarbons (TPH), polycyclic aromatic hydrocarbons (PAHs), and benzene, toluene, ethylbenzene, and xylene (BTEX).

Gas chromatography is the technique adapted to actuate the amounts of TPH in the water specimens. To ascertain the PAHs a standard blend that contains sixteen Polycyclic Aromatic Hydrocarbons was passed down to provide the calibration blend for the specimens. Gas Chromatography-Mass Spectrometer was enabled to test calibration volume standards of the sixteen Polycyclic Aromatic Hydrocarbons, which ranged from 0.01 nanoliter (nL) to 5.00 nanoliter (nL). Using a photo-ionization detector and gas chromatography, BTEX was noticed, and benzene was realized by solvent extraction with tetraethylene glycol. The laboratory techniques for revealing BTEX are notably equivalent to those utilized for revealing PAHs. The outcomes obtained showed a correlation with the target and intervention margin threshold values from the Directorate of Petroleum Resources (DPR 2018).

4. Results and Discussion

4.1 2D ERI Results

The results of 2D electrical resistivity imaging along lines Lx3, Lx5, Ly6, and Ly5 acquired at the spill site are shown in Figures 4 a, b, c, and d.The 2D inverse resistivity sections show low and anomalously high variations in ER revealing a heterogeneous subsurface that is indicative of changing degree of resistivity associated with varying lithology and fluid type.

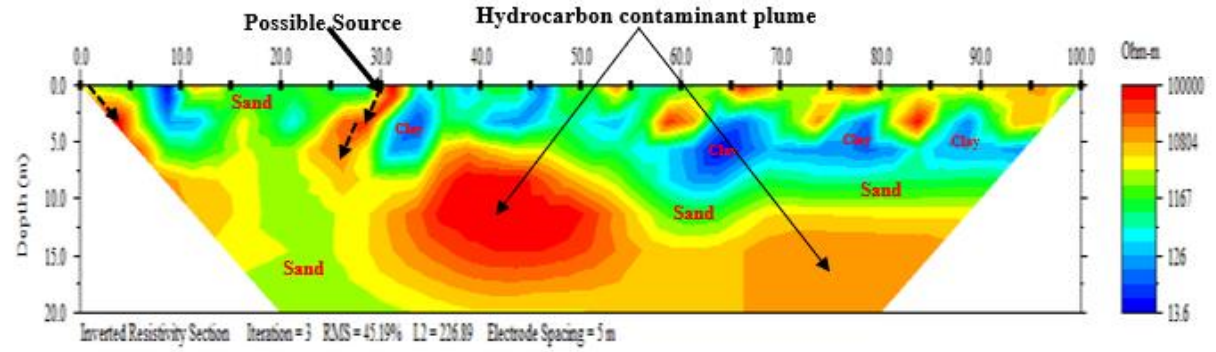

(a) 2D W-S array inverted Resistivity-depth section for line Lx_3

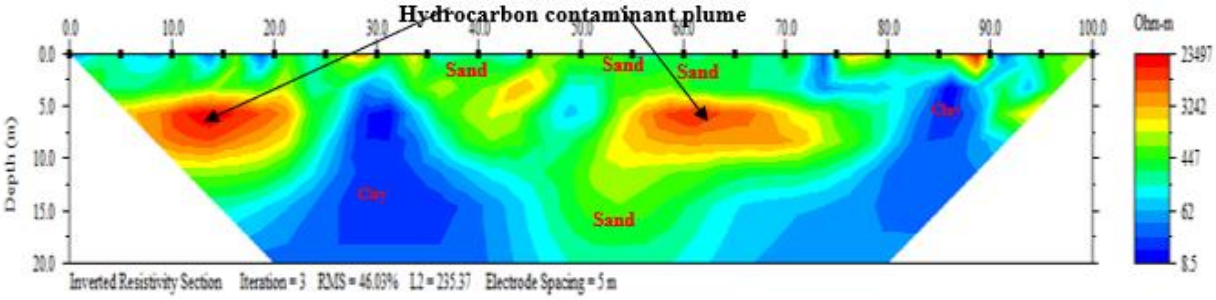

(b) 2D W-S array inverted Resistivity-depth section for line Lx_5

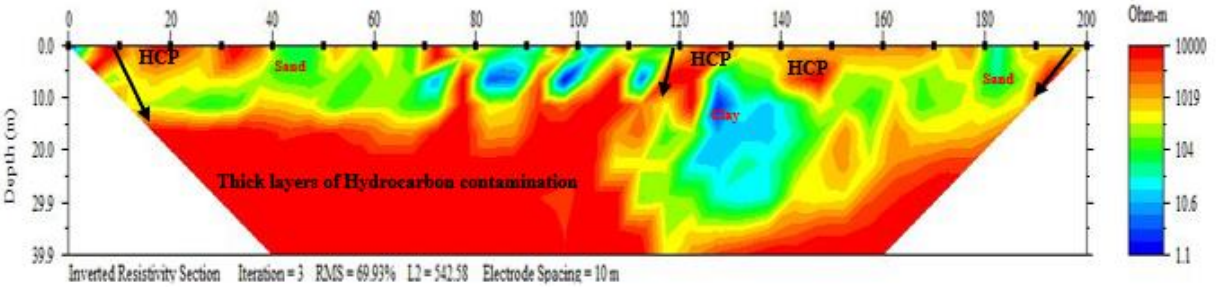

(c): 2D W-S array Inverted Resistivity-depth section for line Ly6 (**HCP: Hydrocarbon contaminant plume**)

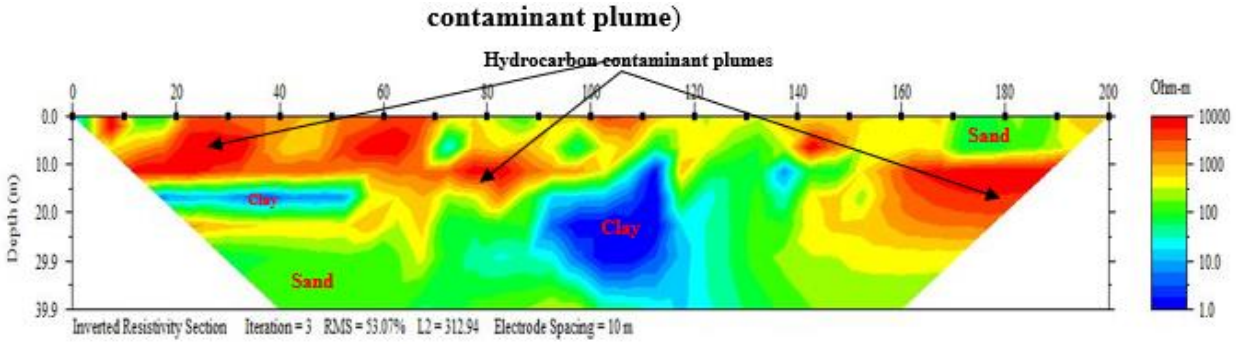

(d): 2D W-S array Inverted resistivity section for line Ly5

Figure 4a-d: 2D ERT Sections for Traverse lines Lx3, Lx5, Ly6, and Ly5 (See Base map of data acquisition)

Resistivity values ranged from 13.6 Ωm to 100,000 Ωm in traverse Lx3 (Figure 4a), 8.5 Ωm to 23,497 Ωm in traverse Lx5 (Figure 4b), 1.1 Ωm to 10,000 Ωm in traverse Ly6 (Figure 4c), and from 1.0 Ωm to 10,000 Ωm in traverse Ly5 (Figure 4d). Layers of high resistivity anomalies exhibiting resistivities between 10,804 Ωm and 100,000 Ωm along line Lx3 (Figure 4a), between 3242 Ωm and 23,497 Ωm along line Lx5 (Figure 4b), between 1019 Ωm and 10,000 Ωm along line Ly6 (Figure 4c), and between 1000 Ωm and 10,000 Ωm along line Ly5 (Figure 4d) extending from the surface (0.0 m) to depths between 10 m and 20 m, and to profound depth of approximately 39.9 m as delineated in traverse line Ly6 (Figure 4c) were observed. These high resistivity structures are indicative of hydrocarbon contamination, because hydrocarbons have a higher electrical resistivity than water. The 2D ERT sections show hydrocarbon contamination with different migration routes, an indication that the source of pollution is a combination of both surface spills, and underground phenomena.

In general, the results of 2D electrical resistivity imaging (ERI) reveal the presence of hydrocarbon contamination in the free-phase at the near-surface (< 5.0 m) to profound depth in a neighborhood of above 20.0 m below the subsurface. Therefore, hydrocarbon pollution has invaded the subsurface down to the water table (approximately about 6.0-7.0 m). The soluble components of hydrocarbon contaminants will be dissolved in the water, and the amount of dissolved solutes was confirmed from geochemical assessment of water samples from boreholes at the oil spill site.

4.2 Geochemical test result of groundwater samples

Groundwater samples from five (5) boreholes (BH-1, BH-2, BH-3, BH-4 and BH-5) at the spill site were utilized to assess the amount of hydrocarbon pollutants in the dissolved phase. Total petroleum hydrocarbons (TPH), polycyclic aromatic hydrocarbons (PAHs), which contain approximately sixteen compounds, and BTEX (benzene, toluene, ethylbenzene, and xylene) are the hydrocarbon contaminants of concern (CoC) examined. This is condensed in Table 2.

Table 2 shows concentrations of TPH in BH-1, BH-2, BH-3, BH-4 and BH-5 as 658.24 µg/L, 610.53 µg/L, 850.03 µg/L, 668.24 µg/L, and 910.53 µg/L, appropriately. The DPR target and intervention thresholds (50 and 600 µg/L) were surpassed by these values as shown in the histogram plot in Figure 5a. The boreholes have a middling TPH of 739.51 µg/L, which exceeds the DPR edge limits. This view hints that the water in the oil spill section encloses an immense level of TPH defilement. Groundwater specimens enclose a summed polycyclic aromatic hydrocarbons (ΣPAHs) at quantities of 0.70 µg/L in BH-1, 0.79 µg/L in BH-2, 0.36 µg/L in BH-3, 1.00 µg/L in BH-4, and 1.89 µg/L in BH-5. Much as these values surpass the DPR target edge of 0.15 µg/L as shown in the histogram plot in Figure 5b, they are enclosed by the intervention edge of 81.50 µg/L. Naphthalene is the prime source of the heightened PAH amounts revealed in the water samples.

Table 2 shows that BH-1 and BH-2 trained naphthalene amounts of 0.35 and 0.65 µg/L, BH-3 retained naphthalene levels of 0.20 µg/L, and BH-4 and BH-5 retained naphthalene levels of 0.44 and 0.73 µg/L, respectively. Boreholes BH-1 to BH-5 had benzene amounts extending from 0.35 to 1.00 µg/L, which surpasses the DPR target edge of 0.20 µg/L (Table 2) nevertheless falls within the intervention margin of 30 µg/L. Toluene concentrations in BH-1, BH-2, BH-3, BH-4, and BH-5 were 0.33 µg/L, 0.19 µg/L, 0.28 µg/L, 0.44 µg/L, and 0.84 µg/L, respectively. Table 2 shows that toluene amounts in BH-1, BH-3, BH-4, and BH-5 were enclosed in the intervention edge of 1000 µg/L but exceeded the DPR target margin of 0.20 µg/L.

Ethylbenzene, m, p-Xylene, and o-Xylene, in addition to all other additional BTEX amounts, had amounts lesser than 0.01 µg/L in BH-1, BH-2, and BH-3, with the exclusion of BH-4 and BH-5, where ethylbenzene levels were 0.09 µg/L and 0.65 µg/L, appropriately, surpassing the DPR target edge of 0.05 µg/L, yet belonging to the intervention edge of 150 µg/L (Table 2). BH-4 and BH-5 possessed m. p-Xylene levels of 0.01 µg/L (below the 0.20 µg/L DPR target edge) and 0.66 µg/L (exceeding the 0.20 µg/L DPR target edge), appropriately. Both amounts prevail under the 70.0 µg/L DPR intervention edge.

Table 2: The findings of the groundwater geochemical appraisal of boreholes from the spill site. The DPR target and intervention standard edges are displayed beside.

Hydrocarbon Contaminants	Units	BH-1	BH-2	BH-3	BH-4	BH-5	DPR	LIMITS
							DPR-T	DPR-I
TPH	µg/l	658.24	610.53	850.03	668.24	910.53	50.00	600.00
PAHs	0	0	0	0	0	0	0	0
Naphthalene	µg/l	0.35	0.65	0.20	0.44	0.73	0	0
Acenaphthylene	µg/l	<0.01	<0.01	<0.01	<0.01	<0.01	0	0
Acenaphthene	µg/l	0.20	<0.01	0.10	0.28	0.31	0	0
Fluorene	µg/l	<0.01	0.06	<0.01	<0.01	0.09	0	0
Anthracene	µg/l	<0.01	<0.01	<0.01	<0.01	<0.01	0	0
Phenanthrene	µg/l	0.02	<0.01	<0.01	0.05	<0.01	0	0
Fluoranthene	µg/l	0.04	<0.01	<0.01	0.07	<0.01	0	0
Pyrene	µg/l	0.09	0.08	<0.01	0.10	0.13	0	0
Benzo (a) anthracene	µg/l	<0.01	<0.01	<0.01	<0.01	<0.01	0	0
Chrysene	µg/l	<0.01	<0.01	0.06	<0.01	0.48	0	0
Benzo (b) fluoranthene	µg/l	<0.01	<0.01	<0.01	0.01	0.15	0	0
Benzo (k) fluoranthene	µg/l	<0.01	<0.01	<0.01	0.01	<0.01	0	0
Benzo (a) pyrene	µg/l	<0.01	<0.01	<0.01	0.01	<0.01	0	0
Dibenz(a,h)anthracene	µg/l	<0.01	<0.01	<0.01	0.01	<0.01	0	0
Indeno(1,2,3-cd) pyrene	µg/l	<0.01	<0.01	<0.01	0.01	<0.01	0	0
Benzo (g,h,i) perylene	µg/l	<0.01	<0.01	<0.01	0.01	<0.01	0	0
Total	0	0.70	0.79	0.36	1.00	1.89	0.15	81.50
BTEX	0	0	0	0	0	0	0	0
Benzene	µg/l	0.84	0.35	0.38	0.95	1.00	0.20	30.00
Toluene	µg/l	0.33	0.19	0.28	0.44	0.84	0.20	1000.00
Ethylbenzene	µg/l	<0.01	<0.01	<0.01	0.09	0.65	0.05	150.00
m. p-Xylene	µg/l	<0.01	<0.01	<0.01	0.01	0.66	0.20	70.00
o-Xylene	µg/l	<0.01	<0.01	<0.01	0.01	0.60	0	0
Total	0	1.17	0.54	0.66	1.50	3.75	0	0

where:

DPR T = Directorate of Petroleum Resources Target values (DPR 2018)

DPR I = Directorate of Petroleum Resources Intervention values (DPR 2018)

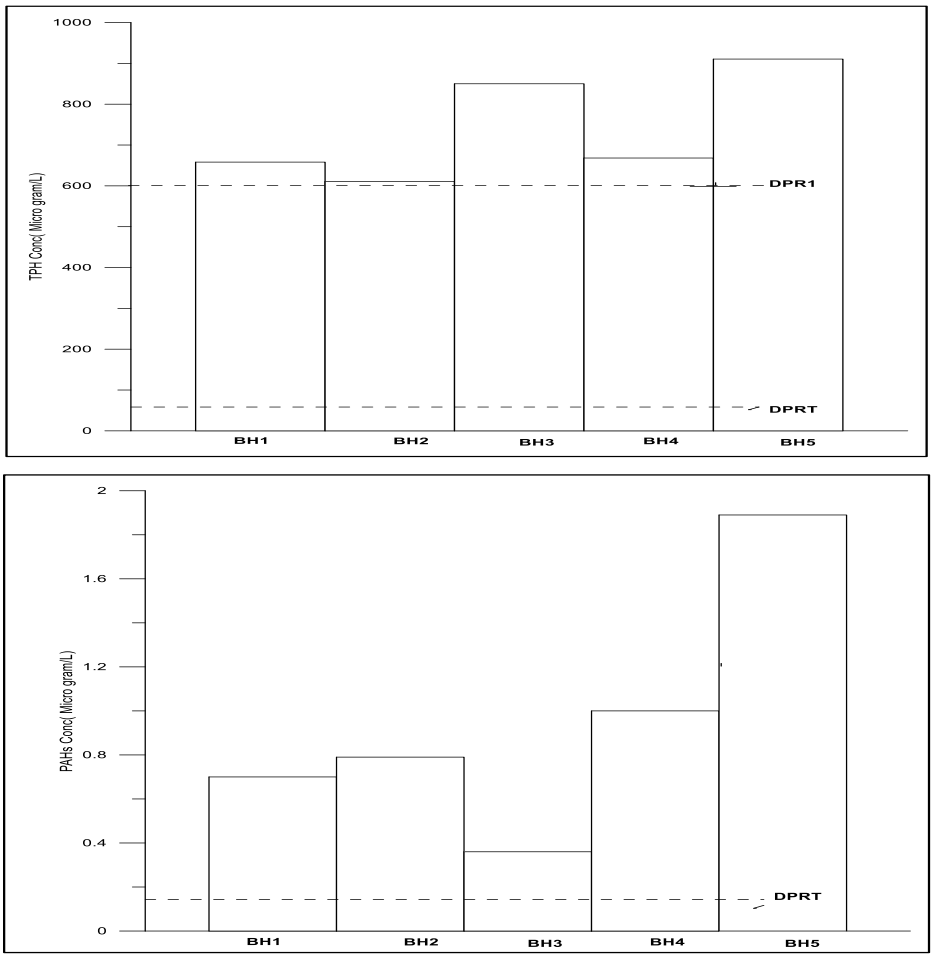

Figure 5: Histogram showing (**a**) total petroleum hydrocarbon (TPH) concentration in groundwater from the five boreholes compared with DPR target and intervention limits (**b**) poly aromatic hydrocarbons (PAHs) concentration in groundwater from the five boreholes compared with DPR target limits.

Groundwater migration route at the spill site was deduced from GMS software program using the calibrated hydraulic head shown in Table 1. The migration route of groundwater at the oil spill site is shown in Figure 5.

In general, groundwater discharges from points of high hydraulic head to low hydraulic head (as indicated by the flow arrows in Figure 5). The dominant flow direction is towards BH_4 located north-west (N-W) of the spill site with BH_1 and BH_5 having higher hydraulic heads, groundwater flow is from BH_1 and BH_5 to the other boreholes (Figure 5). This probably justifies the high values in TPH and PAHs concentrations observed in BH_2, BH_3, and BH_4 (Figure 4 a, b), having received dissolved phase contamination effluents from BH_1 and BH_5. These results are consistent with previous research on hydrocarbon pollution and environmental impact assessment in the Niger Delta as observed in (Nwankwo and Emujakporue, 2012; Eze et al., 2021; Eze et al., 2024).

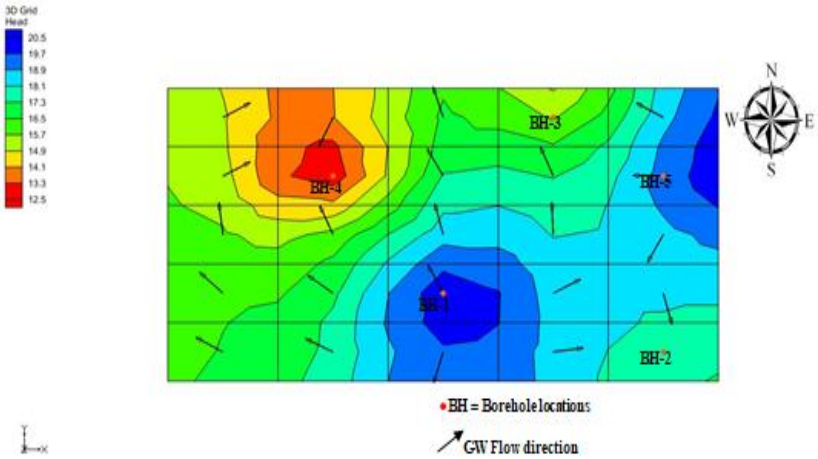

Figure 5: Calibrated hydraulic head distribution showing the groundwater flow at the spill site (arrows indicate the flow direction).

5. Conclusion

In general, the subsurface model for the study area can be characterised by three distinct layers to depths of 20 m and 39.9 m. These layers correspond to clay/sandy clay, sandy layer (which is saturated – possibly contaminated with hydrocarbon in most cases) and a bottom layer composed of sandy clay/clay. The relatively high resistivity obtained for the second layer suggests that this layer has been invaded with hydrocarbon pollution, and it occurs from the near-surface (< 5.0 m) to profound depth between 20 m and 39.9 m. This coincides with the depth of the aquifer that serves as the main source of potable water exploited by the local population. The possible source of contamination differs across the study area varying from surface sources to underground phenomena. Considering the minimum depth of pollution observed from the 2D ERI models the aquifer system below the study area usually exploited for groundwater have been contaminated by hydrocarbon contamination plumes. However, it is important to note that for detailed assessment of hydrocarbon pollution in groundwater at the spill site, geochemical test of water samples from boreholes served as a better proxy for assessment of the amount of dissolved phase contamination in water. The 2D ERI models enabled the

identification of hydrocarbon pollution in the free phase indicated by anomalously high resistivity signatures observed from the surface of the ERI to profound depths below the surface. The groundwater specimens from five boreholes at the spill site were valued to possess a middling total petroleum hydrocarbon (TPH) amount of 739.51 µg/L, beyond the DPR threshold edges. Groundwater specimens with summed polycyclic aromatic hydrocarbons (ΣPAHs) enclosed a range between 0.36 to 1.89µg/L in BH-1 to BH-5, that outweighs the DPR target edge of 0.15 µg/L. Additionally, BTEX levels were observed in greater amounts in the water specimens above the DPR edges. This reveals that the oil spill section contains groundwater that is greatly contaminated by reason of hydrocarbon pollution.

This study has highlighted the effectiveness of integrating geophysical method and geochemical analysis for qualitative and quantitative assessment of hydrocarbon pollution in groundwater. In particular, the utilization of the 2D ERI method has been more effective in this regard, as it provides a better continuous subsurface image and allows for an identification of possible locations of spillage. Although the method is qualitative, 2D ERI is an easy and fast means of obtaining information from the subsurface, the resolution in terms of mapping and identifying hydrocarbon contamination in the free phase greatly aided to characterize the subsurface at the spill site. However, the inversion of 2D ERI data provides a non-unique solution, and geochemical assessment of water samples is useful in constraining data inversion, and has ensured the development of a more reliable data for evaluation of the pollution condition of groundwater at the spill site. A broad characterization of the subsurface as obtained from 2D ERI and geochemical results call for effective remediation planning at the spill site aided by information about the utmost receptor areas at high possibility of contamination which was defined in the groundwater flow pattern at the spill site. The outcomes reached in this study correlates with the result obtained by of similar studies in the region.

Acknowledgements

We are so much thankful to the considerate individuals of the Kegbara Dere community in Ogoniland for letting us entry to the oil spill site to execute the 2D ERI field measurements that were crucial for this investigation.

Availability of data and material Suitable and accessible on request from the corresponding author.

Code availability (Software used)

EarthImager 2D Inv., Grapher-12, Groundwater Modeling System (GMS), and Sufer-13 suite

Funding There was no grant or financial support provided from any agency in the public, commercial, and not-for profit organization for this research work

Declarations

Ethical Approval Not applicable.

Conflicts of interest/Competing interests

The authors declare no conflict of interest.

References

AGI. Earth Imager, 2003. 2-D resistivity inversion software, version 1.5.10. Advanced Geosciences Inc., Austin. Available from: www.agiusa.com/agi-earthimager-2d

Bery, A.A., 2016. Slope monitoring study using soil mechanics properties and 4D electrical resistivity tomography methods. Soil mechanics and foundation engineering, 53 (1), Pp. 24-29.

De Vivo, B., Belkin, H.E., Lima, A., 2008. Environmental geochemistry: Site characterization, data analysis and case histories. Elsevier, The Netherlands Linacre House, Jordan Hill, Oxford OX2 8DP, UK

Doust, H., Omatsola, E., 1990. Niger-Delta. In: Edwards, J.D. and Santogrossi, P.A., Eds., Divergent/Passive Margin Basins, AAPG Memoir 48, American Association of Petroleum Geologists, Tulsa., Pp. 239-248.

Directorate of Petroleum Resources (DPR), 2018. Environmental guidelines and standards for petroleum industry in Nigeria. Revised Annual Reports, Abuja., p. 191. Accessed: Dec 2, 2023

Eze S.U., Ogagarue D.O., Nnorom S.L., Osung W.E., Ibitoye T.A., 2021. Integrated geophysical and geochemical methods for environmental assessment of subsurface hydrocarbon contamination: Environ Monit Assess., 193, Pp. 451. https://doi.org/10.1007/s10661-021-09219-3.

Eze S.U., Ogagarue D.O., Hasan A.K., 2024. Evaluation of 3-D Time-Lapse Electrical Resistivity Tomography and Geochemical Data for Environmental Monitoring And Assessment Of Hydrocarbon Pollution Dynamics. Geosciences Research Journal (GSRJ), 2 (2), Pp. 55-70. Available from: http://doi.org/10.26480/gsrj.02.2024.55.70

Giadom F.D., Akpokodje E.G., Tse A.C., 2015. Determination of migration rates of contaminants in a hydrocarbon-polluted site using non-reactive tracer test in the Niger Delta, Nigeria. Environmental Earth Sciences. 2015; DOI.10.1007/s12665-015-4094-3.

Ideozu R.U., Iheaturu T.C., Ugwueze C.U., Njoku I., 2018. Reservoir

properties and sealing potentials of the Akani Oil Field structures, Eastern Niger Delta, Nigeria. J Oil Gas Petrochem Sci; 1 (2), Pp. 56–65. doi: 10.30881/jogps.00012

Maurya P., Ronde V., Fiandaca G., Balbarini N., Auken E., Bjerg P., Christiansen A., 2017. Detailed landfill leachate plume mapping using 2D and 3D electrical resistivity tomography - with correlation to ionic strength measured in screens. J Appl Geophys., 138, Pp. 1–8.

Nwankwo, C.N., Emujakporue, G.O., 2012. Geophysical method of investigating groundwater and sub-soil contamination-A case study; American Journal of Environmental Engineering, 2 (3), Pp. 49–53 https://doi.org/10.5923/j.ajee. 20120203.02

Obasi, R.A., and Balogun, O., 2001. Water quality and environmental impact assessment of water resources in Nigeria. African Journal of Environment Studies, 2 (2), Pp. 228 – 231.

Okonny I.P., 2002 Geology In Alagoa, E.J. & Derefaka, A (ed) The Land and People of Rivers State, Eastern Niger Delta. Port Harcourt, Onyoma Research Publishers.2002 [cited 2023 Dec 30]

Olaojo A.A., Oladunjoye M.A., Sanuade O.A., 2018. Geoelectrical assessment of polluted zone by sewage effluent in University of Ibadan campus southwestern Nigeria. Environ Monit Assess, 190, Pp. 24. https://doi.org/10.1007/s10661-017-6389-1

Patel S.K., Verma, P., Siggh, G.S., 2019. Agricultural growth and land use land cover change in peri-India, Environ Monit and Assess. 191, Pp. 600. doi:10.100f/s10661-019-7736-1

Pazdirek, O., Blaha, V., 1996. Examples of resistivity imaging using Multi Electrode-100 resistivity field acquisition system. EAGE 58th Conference and Technical Exhibition Extended Abstracts, Amsterdam.

Rivers State Surveyor General Office Report on Ogoniland. 2016. Accessed: Dec. 20, 2023. Available from: http://homepage.ufp/Wiki/climate/page15.html.

Slater, L.D., Sandberg, S.K., 2000. Resistivity and induced polarization monitoring of salt transport under natural hydraulic gradients. Geophysics 65(2):408–420

Tamuno, S., and Felix, J.M. 2006. Crude oil resource: A blessing or curse to Nigeria – The case of the Niger Delta. Journal of Research in National Development 4 (2): 53 – 58

Telford W.M., Geldart L.P., Sheriff R.E. 1990. Resistivity methods In: Applied geophysics, 2nd Edition, (Cambridge Univ. Press, Cambridge, UK) p 353–358. Doi: https://doi.org/10. 1017/cbo9781139167932.012

Uchegbulam O., Ayolabi E.A. 2014. Application of electrical resistivity imaging in investigating groundwater pollution in Sapele area, Nigeria. Journal of water resource and protection. 6:1369-1379.